

Theory of rheology in confinement

Artem A. Aerov and Matthias Krüger

4th Institute for Theoretical Physics, Universität Stuttgart,
Germany and Max Planck Institute for Intelligent Systems, 70569 Stuttgart, Germany*

(Dated: December 7, 2024)

The viscosity of fluids is generally understood in terms of kinetic mechanisms, i.e., particle collisions, or thermodynamic ones as imposed through structural distortions upon e.g. applying shear. Often the former is less relevant, and (damped) Brownian particles are considered good fluid model systems. We formulate a general theoretical approach for rheology in confinement, based on the many particle diffusion equation, evaluated via classical density functional theory. We discuss the viscosity for the situation of two parallel walls in relative motion as a function of wall-to-wall distance.

PACS numbers: 82.70.Dd, 83.80.Hj, 05.70.Ln

The viscosity of fluids is important for scientific research but also for industrial, technological or biological applications. As such, it has been the topic of investigations for many years [1–4], e.g. using linear response theory [5, 6].

A lot is known about rheology of bulk systems. The response of dilute gases [7] can be analyzed starting from kinetic theory [8] such as the Boltzmann equation. For (Brownian) suspensions, insight has been gained, e.g. for dilute systems [9], or glassy ones [10–13]. Here, also non-linear effects are accessible both theoretically and experimentally [14]. While the most fundamental and simplest case concerns bulk systems, improved experimental precision on small scales [15–18] has increased interest in confined systems [19, 20], which is of importance for e.g. microfluidic devices [21, 22], MEMS [23, 24] or blood flow in capillaries [25–27].

Theoretically, a lot of effort has been devoted to gaining control over many body systems [28], where successful (approximate) approaches, based on first principles, include mode coupling theory [10, 29, 30] or density functional theory [31–33]. Using such methods, bulk rheology of dense systems [10, 29, 30] or the time dependence of density profiles under time varying external potentials [32–34] have been studied.

In this Letter, starting from the exact (Smoluchowski) equation of motion [35], we develop a general framework for rheology in confinement, by integrating out particle positions. Using methods of classical density functional theory, we exemplify how simple closures yield the generic behavior of the viscosity in the case of a fluid confined between walls, which had not been accessible by first principles theories before. We discuss how the effective viscosity between two parallel walls depends on the distance between the walls, and on driving velocity, and analyze how it may be understood in terms of a slip length of the fluid at the walls.

Consider a system of N Brownian particles (BPs) and

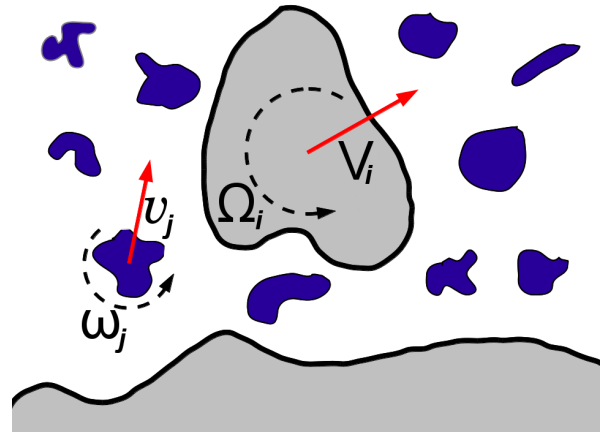


FIG. 1: Model for rheology in confinement: A suspension of (blue) Brownian particles and (gray) non-Brownian particles. The latter are by definition controlled from outside. The forces necessary to maintain the nBPs’ positions and velocities define a general geometry- and shape-dependent viscosity of the fluid.

n non-Brownian particles (nBPs) immersed in a solvent (Fig. 1). The positions and velocities of the nBPs are by construction given, and controlled from outside. This general setup encompasses many realistic situations. For example, cases often termed *microrheology* [36–38], where nBPs of size comparable to the BPs are moved through the fluid. Another important case, considered in detail below, contains two walls moving at a distance comparable to the size of the BPs. Rheological properties of the fluid, which naturally depend among others on size, shape and placement of the nBPs, are captured by the forces necessary to maintain the nBPs’ positions and velocities. Finding these forces is the main goal of this manuscript.

\mathbf{R} (in general $6(n + N)$ dimensional) denotes the particle positions and orientations, and $\mathbf{V} \equiv \partial_t \mathbf{R}$ are the corresponding velocities. Restricting to laminar flow, the resulting hydrodynamic forces, mediated by the solvent, are linear in the velocities, and also instantaneous on the

*Electronic address: aerov@is.mpg.de

time scales considered [39]. They are incorporated in the well known friction or mobility tensors [39]; For the imaginary case, where, in an instant, all velocities are known, the hydrodynamic forces \mathbf{F}^h acting on the $6(n + N)$ degrees of freedom are found from the friction matrix \mathbb{G} ,

$$\mathbf{F}^h = -\mathbb{G}\mathbf{V}. \quad (1)$$

$\mathbb{G} = \mathbb{G}(\mathbf{R})$ is a function of all particle coordinates. If –considering another imaginary situation– all forces \mathbf{F}_N driving the BPs are known, the mobility tensor \mathbb{M} yields their velocities \mathbf{V}_N ,

$$\mathbf{V}_N = \mathbb{M}\mathbf{F}_N. \quad (2)$$

By definition, the nBPs are excluded from \mathbb{M} since their velocities are prescribed. \mathbb{M} is thus a $6N$ dimensional matrix, however still depending on all positions, $\mathbb{M} = \mathbb{M}(\mathbf{R})$. Mathematically, it is the inverse of \mathbb{G} after projection on the subspace spanned by the BPs. Above and in the following, we use subscripts to denote dimensionality of vectors and matrices, e.g. \mathbf{V}_N is spanned by the subspace of BPs, and \mathbb{G}_{Nn} (see e.g. Eq. (4) below) is a matrix transforming from the nBPs' subspace to the BPs' one.

Direct forces are given in terms of the potential $W(\mathbf{R})$. The first step will be finding the (time dependent) probability distribution $P(\mathbf{R}_N, t)$ for the Brownian degrees of freedom, which follows from force balance. On the Brownian time scale [39], where momenta have relaxed, the total force on the BPs vanishes,

$$0 = (\mathbb{G}\mathbf{V})_N + \nabla_N [W + k_B T \ln P]. \quad (3)$$

Here, the first term is the hydrodynamic force due to motion of particles, and the second term is the potential force. The last term $\propto \nabla_N \ln P$ (the so-called Brownian force [39]) is a well known mathematical expression useful for a short route to the Smoluchowski equation (Eq. (5) below). Physically, it captures (entropic) forces due to thermal fluctuations. The Smoluchowski equation is found from solving Eq. (3) for \mathbf{V}_N ,

$$\mathbf{V}_N = -\mathbb{M}(\nabla_N [W + k_B T \ln P] + \mathbb{G}_{Nn}\mathbf{V}_n), \quad (4)$$

and requiring continuity [33, 39], i.e., $\frac{\partial}{\partial t}P = -\nabla \cdot \mathbf{V}_N P$,

$$\frac{\partial}{\partial t}P = \nabla \cdot \mathbb{M}(\nabla_N [W + k_B T \ln P] + \mathbb{G}_{Nn}\mathbf{V}_n)P. \quad (5)$$

Eq. (5) yields $P(\mathbf{R}_N, t)$, by itself a quantity of interest, measurable e.g. by use of confocal microscopy. With it, any (time dependent) observable is accessible in this framework, e.g. mean squared displacements. Here, we focus on the rheological properties of the fluid, which are most generally expressed in terms of the forces necessary to maintain positions and velocities of the nBPs.

In order to find these forces, it is important to note that the velocities of BPs are a direct function of their positions and the distribution P , see Eq. (4). The mean force \mathbf{F}_n (balancing the external one) acting on the nBPs, as measured on the Brownian time scale, is hence

$$\langle \mathbf{F}_n \rangle(t) = -\int d\mathbf{R}_N P(t) [\mathbb{G}_{nn}\mathbf{V}_n + \mathbb{G}_{nN}\mathbf{V}_N + \nabla_n W]. \quad (6)$$

The first term on the rhs of Eq. (6) is the force induced by the motion of the nBPs. Here, \mathbb{G}_{nn} can be seen as an effective friction matrix of the complex fluid. The second term contains the force on the nBPs due to the motion of BPs. The last term is the potential force, also depending on the positions of BPs, and hence part of the integral.

The force in (6) depends on the velocities and positions of nBPs at time t , but generally also on their trajectories in the past. While in Eq. (6) we give the mean force, higher moments, e.g. fluctuations of the force [37], are accessible as well once P is known.

Solving Eq. (5) is challenging in general, and exact solutions have in most cases been restricted to $N = 2$, see e.g. Ref. [9]. We will proceed by making Eqs. (5) and (6) amenable to (approximate) treatments via classical density functional theory [31]. Thereby, we restrict to spherical BPs, which interact with a pairwise potential $\phi(\mathbf{r}_{ij})$, depending only on the respective center-center-distance \mathbf{r}_{ij} . More specifically, we decompose $W(\mathbf{R}) = U(\mathbf{R}_n) + \sum_{i=1}^N V(\mathbf{r}_i, \mathbf{R}_n) + \sum_{j \neq i} \sum_{i=1}^N \phi(\mathbf{r}_{ij})$. Furthermore, as regards the BPs, we restrict to pairwise hydrodynamic interactions as well, which simplifies the matrices \mathbb{G} and \mathbb{M} . Integrating over $N - 2$ particle positions, we obtain the following equation for the time evolution of the one body density $\rho(\mathbf{r}, t)$,

$$\frac{\partial \rho(\mathbf{r}_1)}{\partial t} = \nabla_1 \cdot \int d\mathbf{r}_2 \mathbf{J}(\mathbf{r}_1, \mathbf{r}_2). \quad (7)$$

Here, we introduced the two-particle current \mathbf{J} ,

$$\mathbf{J}(\mathbf{r}_1, \mathbf{r}_2) \equiv \delta(\mathbf{r}_2) \mathbf{j}^{(1)}(\mathbf{r}_1) + \mathbf{j}^{(2)}(\mathbf{r}_1, \mathbf{r}_2) = \delta(\mathbf{r}_2) \rho(\mathbf{r}_1) \mathbb{M}_{11}^{(1)} \left[\mathbf{F}_1 + \mathbb{G}_{1n}^{(1)} \mathbf{V}_n \right] + \rho^{(2)}(\mathbf{r}_1, \mathbf{r}_2) \left[\mathbb{M}_{12}^{(2)} \mathbf{F}_2 + (\mathbb{M}\mathbb{G})_{1n}^{(2)} \mathbf{V}_n \right]. \quad (8)$$

The force $\mathbf{F}_1(\mathbf{r}) = \nabla [k_B T \ln \rho(\mathbf{r}) + V] + \rho^{-1}(\mathbf{r}) \int d\mathbf{r}' \rho^{(2)}(\mathbf{r}, \mathbf{r}') \nabla \phi(\mathbf{r} - \mathbf{r}')$ is an effective one body force [33], and we denote $\mathbf{F}_2 = (\mathbf{F}_1(\mathbf{r}_1), \mathbf{F}_1(\mathbf{r}_2))^T$, a six dimensional vector [47], and $\rho^{(2)}(\mathbf{r}_1, \mathbf{r}_2)$ is the two-particle density [28]. Furthermore, upper index (i) denotes a hydrodynamic tensor depending on the positions of i BPs. [48] Finally we note that removing all nBPs, Eqs. (7) and (8) can be identified with Eq. (2) in Ref. [34]. The force acting on the

nBPs follows accordingly from integrating Eq. (6) [49],

$$\langle \mathbf{F}_n \rangle = \mathbf{F}_n^{\rho=0} + \int d\mathbf{r}_1 d\mathbf{r}_2 \left[\delta(\mathbf{r}_2) \rho(\mathbf{r}_1) \left[\nabla V(\mathbf{r}_1) - \mathbb{G}_{nn}^{(1)}(\mathbf{r}_1) \mathbf{V}_n \right] + \mathbb{G}_{nn}^{(1)}(\mathbf{r}_1) \mathbf{J} + \rho^{(2)} \left(\mathbb{G}_{nn}^{(2)} \left[\frac{\mathbf{j}^{(1)}(\mathbf{r}_1)}{\rho(\mathbf{r}_1)} + \mathbf{j}^{(2)} \right] - \mathbb{G}_{nn}^{(2)} \mathbf{V}_n \right) \right]. \quad (9)$$

In Eq. (9), $\mathbf{F}_n^{\rho=0} = -\nabla_n U(\mathbf{R}_n) - \mathbb{G}_{nn}^{(0)} \mathbf{V}_n$ denotes potential and hydrodynamic forces in absence of BPs.

We note that the more familiar drift diffusion equation [36, 39], or the Smoluchowski equation for shear where hydrodynamic interactions are neglected [39], follows from Eqs. (5) or (8) by replacing $\mathbb{M}_{11}^{(1)} = D_0/k_B T$ to leading order and $-\mathbb{M}_{11}^{(1)} \mathbb{G}_{1n}^{(1)} \mathbf{V}_n = \mathbf{V}(\mathbf{r})$, the solvent velocity induced by the moving nBPs.

Let us consider the simple but important case of two parallel walls moving with respect to each other (see the inset of Fig. 2), a scenario accessible by experiments and simulations [19, 40]. We place the lower wall in the plane $y = 0$, and the upper in the plane $y = d$. The upper wall moves deterministically with velocity v along direction x , defining a bare shear rate of $\dot{\gamma}_0 = \frac{v}{d}$. The upper wall is subject to the force $\mathbf{F}^{(u)}$ found from Eq. (9). Due to symmetries, it has no component along z , and its components along y and x yield the orthogonal pressure and the shear viscosity, respectively. Focusing on the latter, we define the effective viscosity of the confined fluid ν_{eff} in terms of the x -component of $\mathbf{F}^{(u)}$, which, in the considered stationary situation is time independent,

$$\nu_{\text{eff}} = \frac{F_x^{(u)}}{A \dot{\gamma}_0}. \quad (10)$$

Here, A is the surface area of the plate [note that $F_x^{(u)}/A$ may as well be identified with the shear stress]. Eqs. (8) and (9) can be evaluated to any order of (pairwise) hydrodynamic interactions, and it is instructive to introduce BPs with hydrodynamic radius $a_H/2$ and hard interaction radius $a/2$, as then, for $a_H < a$, convergence of a series in a_H/a may be assumed. In zeroth order, the BPs are infinitely fast, and their density distribution adjusts instantaneously to the equilibrium distribution corresponding to the arrangement \mathbf{R}_n of nBPs at time t . This is explicitly found from Eq. (7), which to zeroth order requires $\mathbf{F}_1 = 0$, as fulfilled by ρ_{eq} [28]. In this order, the effective viscosity in Eq. (10) is given by the bare solvent viscosity ν_0 . In general,

$$\nu_{\text{eff}} = \nu_0 + \nu_1 a_H + \nu_2 a_H^2 + \dots \quad (11)$$

ν_1 , ν_2 and so on, depend nontrivially on the distance d [as well as on velocity v and average density]. In order to compute them, $\rho^{(2)}$ in Eqs. (8) and (9) must be expressed in terms of ρ . As demonstrated in Ref. [41], a simple closure involving the distorted bulk pair distribution $g_{neq}(\mathbf{r}) \equiv g(\mathbf{r}) - g_{eq}(\mathbf{r})$ under shear suffices to capture the distortion of $\rho^{(2)}$ necessary for shear cases,

$$\rho^{(2)}(\mathbf{r}, \mathbf{r}') \approx \rho_{ad}^{(2)}(\mathbf{r}, \mathbf{r}') + \rho(\mathbf{r})\rho(\mathbf{r}')g_{neq}(\mathbf{r} - \mathbf{r}'). \quad (12)$$

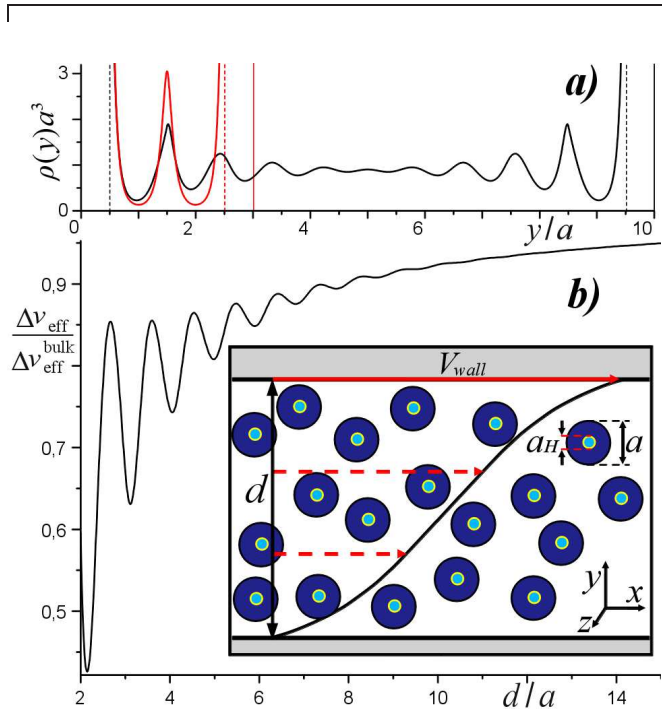


FIG. 2: b) Effective viscosity $\Delta\nu_{\text{eff}} = \nu_{\text{eff}} - \nu_0$ of a suspension sheared between walls, as a function of the distance d between them, normalized to the bulk value for large d . The average Packing fraction is $\Phi = 0.45$, and we consider particles with small hydrodynamic radii (see inset sketch). Part a) gives the corresponding equilibrium densities for two exemplary cases, $d = 10$ and $d = 3$ (compare Ref. [44]). Solid vertical lines denote the position of the walls, while the vertical dashed ones give the closest approach for particle centers.

Here, $\rho_{ad}^{(2)}$ is the so-called adiabatic term, which is expressed via the density functional, and is the main ingredient of dynamical density functional theory [33]. We use the Rosenfeld functional for this term. The second term in Eq. (12) is the addition necessary to capture effects of shear [41, 42]. By definition, Eq. (12) is exact in homogeneous systems, and uses knowledge about bulk rheology [14], imprinted in $g_{neq}(\mathbf{r})$, to describe effects in inhomogeneous situations. Eq. (12) is readily amenable to expansion in a_H , where the results for g_{neq} are taken from [9]. We note that the general search for closures of Eq. (5) will also benefit from recent fundamental developments in dynamical density functional theory [43].

Fig. 2 b) shows the resulting viscosity for hard spheres of average packing fraction $\Phi = 0.45$ [50], confined by hard walls. Specifically, the curve gives the coefficient ν_1 in Eq. (11), normalized by its bulk value. By construction, the curve approaches unity for large d , and, in the limit of small d/a , in tendency reduces to smaller values.

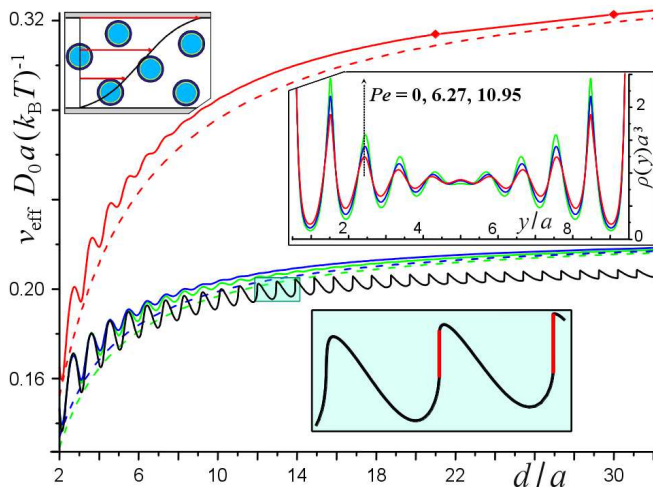


FIG. 3: Effective viscosity of a hard sphere fluid sheared between two walls as a function of the distance d between them for $Pe = 0, 6.27, 10.95, 20$ (full curves, top to bottom). Dashed curves represent corresponding estimates via the slip length computed for an isolated wall, Eq. (13). Inset shows enlarged segment of the lowest curve, where discontinuities as a function of d develop. $\Phi = 0.45$.

While the curve is smooth for $d \gtrsim 8a$, it develops oscillations for smaller d , which are due to layering effects, that are more pronounced at smaller d , as seen in panel a).

While Fig. 2 represents the case of small a_H , the observed qualitative scenario is more general, as we aim to demonstrate by use of a model implemented in Ref. [41] for the case of one wall. Here, hydrodynamic interactions are included effectively, by introduction of an average solvent velocity $\langle \mathbf{v} \rangle$, and hydrodynamic forces acting on the BPs are computed as $\mathbf{F}_N^h D_0 / k_B T = \langle \mathbf{v} \rangle - \mathbf{V}_N$. The model then adjusts the mean velocity $\langle \mathbf{v} \rangle(y)$, thereby achieving stress homogeneity as required by stationarity. The local stress is an exact functional of $\rho^{(2)}$ [8], and self-consistently found [41]. We note that this model exactly agrees with Eqs. (8) and Eq. (9) for small a_H , while it easily allows consideration of the case $a_H = a$. Furthermore, due to its simplicity, the model may capture generic features independent of system details.

Fig. 3 shows the resulting effective viscosity (see Eq. (10)) for different Peclet numbers $Pe \equiv \dot{\gamma}_0 a^2 / D_0$. The upper curve shows the case of small Pe , i.e. linear response. It indeed possesses very similar features as compared to Fig. 2: The effective viscosity approaches a distance independent bulk value for $d \rightarrow \infty$, while it consistently reduces to smaller values for small d . Again, for $d \lesssim 8a$, oscillations start to be visible.

In Ref. [41], using the same model, we computed a slip length L of the suspension at a single wall under shear. A geometrical consideration suggests the following effective viscosity for the case of two parallel walls at distance d ,

$$\nu_{\text{eff}}(d) = \nu_{\text{eff}}(d \rightarrow \infty) \frac{d}{d + 2L}, \quad (13)$$

a function of L and the viscosity for large d (bulk). The outcome of Eq. (13) is shown in Fig. 2 by dashed curves, where for small Pe , we have $L = 1.27$ [41]. Despite the mentioned oscillations in the solid curve, which are not reflected by Eq. (13), Eq. (13) gives an astonishingly good result for d as small as 2 particle diameters. We note that e.g. for $d = 3a$, the density shown in Fig. 2 a) is rather inhomogeneous, while the effective viscosity is still well described by the estimate of Eq. (13). Once the distance is decreased even further, details of the walls may possibly influence the effective viscosity (e.g. surface roughness or lubrication forces), which are beyond the scope of the present paper.

Upon increasing the driving velocity, the asymptote for large d decreases, which is due to the well known phenomenon of shear thinning in bulk systems at intermediate values of Pe . Apart from this, the overall qualitative features are very similar to the discussed cases, in particular, Eq. (13) gives a very good estimate of the overall trend for larger rates as well. Regarding $Pe = 10.95$, we see that the oscillations in the viscosity extend to larger values of d . This is a clearly non-linear effect, as the higher rate causes changes in the density (see inset of Fig. 3), which for increasing rates develops more pronounced oscillations, extending to larger d .

As found in simulations [45, 46], bulk suspensions show layering for certain densities and shear rates. The behavior of the viscosity in confinement is hence nontrivial. The considered model [41, 42] shows a layering instability for large Peclet numbers, upon which the one-particle density develops oscillations along y for arbitrarily large distances d . The lowest curve of Fig. 3 shows a state in which the bulk is layered ($Pe = 20$). In that case, we see that the effective viscosity is *unsteady* as a function of d , showing discrete jumps for $d \gtrsim 12a$, which can be understood by the underlying density profiles. At the jumps of $\nu_{\text{eff}}(d)$, the density is discontinuous as well, as the number of layers is changed by one. Our analysis thus predicts that this discontinuity is also found in the viscosity. Last, we note that the relative height of the discontinuities decays as $1/d$, since for large d each individual layer contributes less to the total viscosity.

Exemplified by monodisperse hard spheres, the viscosity of fluids in confinement displays a variety of features. In the case of two walls in relative motion, the viscosity is astonishingly well described by a continuum estimate involving the slip length, Eq. (13), down to distances of a few particle diameters. According to the estimate, at large distances, the viscosity approaches the bulk value with a correction vanishing as $1/d$. At distances of a few particle diameters, the viscosity additionally displays oscillations as a function of distance. At larger driving velocities, nonlinear effects are present, e.g. the oscillatory behavior of viscosity is extended to larger distances.

We thank J. M. Brader, R. Evans, M. Fuchs and J. Wu for useful discussions. This research was supported by Deutsche Forschungsgemeinschaft (DFG) grant No. KR 3844/2-1.

-
- [1] J. Maxwell, Philosophical Transactions of the Royal Society of London **156**, 249 (1866).
- [2] D. S. Viswanath, T. K. Ghosh, D. H. L. Prasad, N. V. K. Dutt, and K. Y. Rani, Viscosity of Liquids (Springer, The Netherlands, 2007).
- [3] W. D. Monnery, W. Y. Svrcek, and A. K. Mehrotra, The Canadian Journal of Chemical Engineering **73**, 340 (1995).
- [4] E. Elliott, J. Joseph, and J. Thomas, Phys. Rev. Lett. **113**, 020406 (2014).
- [5] M. Green, J. Chem. Phys. **20**, 1281 (1952).
- [6] R. Kubo, J. Phys. Soc. Jpn. **12**, 570 (1957).
- [7] E. da C. Andrade, London Edinb. Dub. Philos. Mag. J. Sci. **17(112)**, 497 (1934).
- [8] H. J. Kreuzer, Nonequilibrium thermodynamics and its statistical foundations (Clarendon press, Oxford, 1981).
- [9] J. Brady and J. Morris, J. Fluid. Mech. **348**, 103 (1997).
- [10] M. Fuchs and M. E. Cates, Phys. Rev. Lett. **89**, 248304 (2002).
- [11] P. Sollich, F. Lequeux, P. Hébraud, and M. E. Cates, Phys. Rev. Lett. **78**, 2020 (1997).
- [12] M. L. Falk and J. S. Langer, Phys. Rev. E **57**, 7192 (1998).
- [13] A. Nicolas and J.-L. Barrat, Faraday Discuss. **167**, 567 (2013).
- [14] J. Brader, J. Phys.: Condens. Matter **22**, 363101 (2010).
- [15] F. V. Ignatovich and L. Novotny, Phys. Rev. Lett. **96**, 013901 (2006).
- [16] L. Isa, R. Besseling, A. N. Morozov, and W. C. K. Poon, Phys. Rev. Lett. **102**, 058302 (2009).
- [17] X. Cheng, J. H. McCoy, J. N. Israelachvili, and I. Cohen, Science **333**, 1276 (2011).
- [18] T. Chevalier, S. Rodts, X. Chateau, C. Chevalier, and P. Coussot, Phys. Rev. E **89**, 023002 (2014).
- [19] J. Petracic and P. Harrowell, J. Chem. Phys. **124**, 044512 (2006).
- [20] S. H. L. Klapp, Y. Zeng, D. Qu, and R. von Klitzing, Phys. Rev. Lett. **100**, 118303 (2008).
- [21] D. Psaltis, S. R. Quake, and C. Yang, Nature **442**, 381 (2006).
- [22] P. Sajeesh and A. K. Sen, Microfluid Nanofluid **17**, 1 (2014).
- [23] C.-M. Ho and Y.-C. Tai, Annu. Rev. Fluid Mech. **30**, 579 (1998).
- [24] B.-Y. Cao, J. Sun, M. Chen, and Z.-Y. Guo, Int. J. Mol. Sci. **10**, 4638 (2009).
- [25] K. Boryczko, W. Dzwiniel, and D. A. Yuen, J. Mol. Model. **9**, 16 (2003).
- [26] H. Li, H. Fang, Z. Lin, S.X. Xu, and S. Chen, Phys. Rev. E **69**, 031919 (2004).
- [27] J. Zhou and H. C. Chang, J. Colloid Interface Sci. **287**, 647 (2005).
- [28] J.-P. Hansen and I. McDonald, Theory of simple liquids (Academic Press, 2009).
- [29] J. Brader, T. Voigtmann, M. Fuchs, R. Larson, and M. Cates, Proc. Natl. Acad. Sci. U.S.A. **106**, 15186 (2009).
- [30] K. Miyazaki and D. R. Reichman, Phys. Rev. E **66**, 050501 (2002).
- [31] R. Evans, Adv.Phys. **28**, 143 (1979).
- [32] U. M. B. Marconi and P. Tarazona, J. Chem. Phys. **110**, 8032 (1999).
- [33] A. J. Archer and R. Evans, J. Chem. Phys. **121**, 4246 (2004).
- [34] M. Rex and H. Löwen, Phys. Rev. Lett. **101**, 148302 (2008).
- [35] H. Risken, The Fokker-Planck Equation (Springer, Berlin, 1984).
- [36] M. Rauscher, A. Dominguez, M. Krüger, and F. Penna, J. Chem. Phys. **127**, 244906 (2007).
- [37] T. M. Squires and J. F. Brady, Phys. Fluids **17**, 073101 (2005).
- [38] L. G. Wilson, A. W. Harrison, W. C. K. Poon, and A. M. Puertas, Eur. Phys. Lett. **93**, 58007 (2011).
- [39] J. K. G. Dhont, An Introduction to Dynamics of Colloids (Elsevier science, Amsterdam, 1996).
- [40] P. Peyla and C. Verdier, Eur. Phys. Lett. **94**, 44001 (2011).
- [41] A. A. Aerov and M. Krüger, J. Phys. Chem. **140**, 094701 (2014).
- [42] J. Brader and M. Krüger, Mol. Phys. **109**, 1029 (2011).
- [43] M. Schmidt and J. M. Brader, J. Chem. Phys. **138**, 214101 (2013).
- [44] B. Götzelmann and S. Dietrich, Phys. Rev. E **55**, 2993 (1997).
- [45] S. R. Rastogi, N. J. Wagner, and S. R. Lustig, J. Chem. Phys. **104**, 9234 (1996).
- [46] D. R. Foss and J. F. Brady, J. Rheol. **44**, 629 (2000).
- [47] To obtain Eq. (8), we used the first two members of the the Yvon-Born-Green relations [28] to approximate $\rho^{(3)}$.
- [48] E.g., $\mathbb{M} = \sum_{l=1}^N \left(\mathbb{M}_{11}^{(1)}(\mathbf{r}_l) + \sum_{k \neq l}^N \mathbb{M}_{12}^{(2)}(\mathbf{r}_l, \mathbf{r}_k) + \dots \right)$,
 $\mathbb{M}\mathbb{G}_{\mathbf{N}\mathbf{n}} = \sum_{l=1}^N \left(\mathbb{M}_{11}^{(1)}\mathbb{G}_{1\mathbf{n}}^{(1)}(\mathbf{r}_l) + \sum_{k \neq l}^N (\mathbb{M}\mathbb{G})_{1\mathbf{n}}^{(2)}(\mathbf{r}_l, \mathbf{r}_k) + \dots \right)$
- [49] We collected all terms involving ρ and $\rho^{(2)}$.
- [50] In contrast to equilibrium cases [31, 44], which are naturally discussed grand canonically, we prefer to keep the particle packing fixed, thus avoiding the definition of a chemical potential in non-equilibrium.